Tunable nanoporosity in Sr-doped ZnO thin films by thermal annealing treatment and its effect on photocatalytic activity

LINHUA XU[a,b,c,*], FENGLIN XIAN[a,b], YULIN CHEN[a], JUHONG MIAO[a], JING SU[a], SHIXIN PEI[a], FANG GU[a], LIMING QIAN[a]

[a]*School of Physics and Optoelectronic Engineering, Nanjing University of Information Science & Technology, Nanjing 210044, China*

[b]*Optics and Photonic Technology Laboratory, Nanjing University of Information Science & Technology, Nanjing 210044, China*

[c]*Jiangsu Research Center for Ocean Survey Technology, Nanjing University of Information Science & Technology, Nanjing 210044, China*

In this work, Sr-doped ZnO thin films are prepared by sol-gel technique and annealed at various temperatures. The crystal structure of the samples is analyzed by X-ray diffraction (XRD); surface and sectional morphologies are observed by scanning electron microscopy (SEM). The XRD patterns show that all the films crystallize in a wurtzite phase and have a preferential orientation along the c-axis. The SEM morphology images reveal that all the Sr-doped ZnO thin films have a porous structure and the pore size changes with the rise of annealing temperature. When the annealing temperature is 500 ℃, the porosity in the films is highest. The photocatalytic tests of these samples show that all th e porous ZnO thin films exhibit better photocatalytic performance than pure ZnO thin films; and the sample annealed at 500 ℃ exhibits the highest photocatalytic activity, which should be attributed to the higher porosity and stronger light absorption.

(Received November 23, 2015; accepted February 10, 2017)

Keywords: Porous ZnO thin films; Annealing temperature; Sol-gel method; Photocatalytic activity

1. Introduction

In recent years, the industry in some developing countries gains rapid development, but at the same time, the serious environmental pollution has been made due to lack of environmental protection consciousness or related environmental protection techniques. The environmental pollution mainly includes air and water pollution; and the water pollution is more serious in most countries. For example, many rivers and lakes in China have been polluted by industrial wastewater so that the water in them is no longer able to be drunk and irrigated directly. Therefore, how to effectively solve these environmental pollution problems has received widespread attention. Nowadays, the photocatalytic technique as a new method to tackle the environmental pollution problems has been paid much attention in many countries because it utilizes solar energy and almost does not produce pollutants. The semiconductor photocatalyst is the key factor in the photocatalytic technique. The widely investigated photocatalysts currently include TiO_2, ZnO, SnO_2, Fe_2O_3, and so on. Among these semiconductor photocatalysts, ZnO is the most investigated material after TiO_2 [1-7]. This is because ZnO has a comparable photocatalytic performance to TiO_2; even in some cases, ZnO nanomaterials have a better photocatalytic performance than TiO_2 nanomaterials [8, 9]. Furthermore, ZnO nanomaterials are easily prepared by some facile methods.

ZnO nanoparticle is the most widely used photocatalyst form for ZnO materials. Because nanoparticles possess high specific surface area, lots of surface active sites and strong light-absorption ability, ZnO nanoparticles usually exhibit excellent photocatalytic activity [10-14]. However, these nanoparticles are hard to be separated from water after photocatalytic degradation is finished, which is possible to cause a second pollution. Thus, exploring substrate-supported ZnO materials like ZnO thin films as photocatalysts is an inevitable choice [15-17]. Compared with ZnO nanoparticles, although ZnO thin films are easily separated from liquid and to be recycled, they also have some inevitable shortcomings, such as low specific surface area, reduced light-absorption ability, smaller probability for photoinduced carriers inside the films to migrate to film surface to react with pollutants,

etc. These shortcomings deteriorate the photocatalytic performance of ZnO thin films to some extent. In order to improve the photocatalytic activity of ZnO thin films, some methods are adopted including doping other ions in ZnO thin films [18, 19], surface modifications [20], forming composite thin films with other materials [21], making porous structure in ZnO films [22, 23], etc. Among these methods, the relatively facile and cost-effective method is the last one, and the porous ZnO thin films also displayed high photocatalytic activity [22]. Therefore, to develop porous ZnO thin films with low production cost, high photocatalytic activity and good reusability becomes a hot research topic [24].

In this study, Sr-doped ZnO thin films were prepared and annealed at different temperatures. It was found that annealing temperature had a great effect on the porosity. The change of the porosity in turn influenced the photocatalytic activity of the ZnO films. The details about the evolution of the porosity with the increase of annealing temperature as well as the photocatalytic activity of the films were described below.

2. Experiments

Sr-doped ZnO thin films were deposited by sol-gel method. Firstly, a ZnO sol was prepared using zinc acetate, strontium chloride, anhydrous alcohol, monoethanolamine as precursor, dopant, solvent and stabilizer, respectively. The molar ratio of Sr/Zn is 0.02 in the sol. The sealed ZnO sol was aged in dark for 24 hours, and then Sr-doped ZnO thin films were deposited by spin-coating the sol on glass and Si substrates. The as-prepared Sr-doped ZnO thin films were annealed respectively at 400, 450, 500 and 550 ℃ for one hour. Since that the glass substrates will be deformed badly when the annealing temperature is beyond 550 ℃, there is no higher temperature annealing treatment to be performed. Under the same conditions, a pure ZnO thin film was prepared and annealed at 500 ℃ for one hour.

The crystal structures of the samples were determined by an X-ray diffractometer (Bruker D8 Advance).The surface and section morphology of the samples was observed by a field emission scanning electron microscope (S-4800). The chemical composition of the films was analyzed by an energy dispersive X-ray spectrometer attached to the SEM. The transmittance of the films and the absorbance of methylene blue aqueous solution were recorded by a spectrophotometer (TU-1901).

The photocatalytic activity of the films was tested using the methylene blue (MB) as a simulated pollutant. The concentration of methylene blue in aqueous solution is 5 mg/L; the effective area of the films is 1.5×1.5 cm^2; the light source is an Hg lamp. Before a photocatalytic test, the MB solution containing a ZnO thin film was placed in the dark for 30 min to allow adsorption-desorption equilibrium; then the solution was exposed to light irradiation. At an interval of 20 min, the absorbance at 664 nm of the MB solution would be measured to decide the degradation rate of MB in the solution. The degradation rate was calculated by the following formula:

$$\eta = \frac{C_0 - C}{C_0} \times 00\% = \frac{A_0 - A}{A_0} \times 00\% \qquad (1)$$

Where η is degradation rate, C_0 and A_0 is the MB concentration and absorbance before light irradiation, C and A is the MB concentration and absorbance after the solution is exposed to light irradiation for 120 min.

3. Results and discussion

3.1. The crystal structures and morphology features of the ZnO thin films

Fig. 1 shows the XRD patterns of the Sr-doped ZnO thin films annealed at different temperatures. All the diffraction peaks in the patterns can be indexed to wurtzite structured ZnO, indicating the ZnO samples have a pure phase. The strong (002) peak **suggests** that the ZnO thin films are preferentially oriented along the c-axis direction perpendicular to the substrate surface. With the increase of annealing temperature, the (002) peak is gradually enhanced and its full width at half maximum is decreased, indicating the crystalline quality of the films is improved and the ZnO crystal size is increased. The similar results have been also reported by others [25-27].

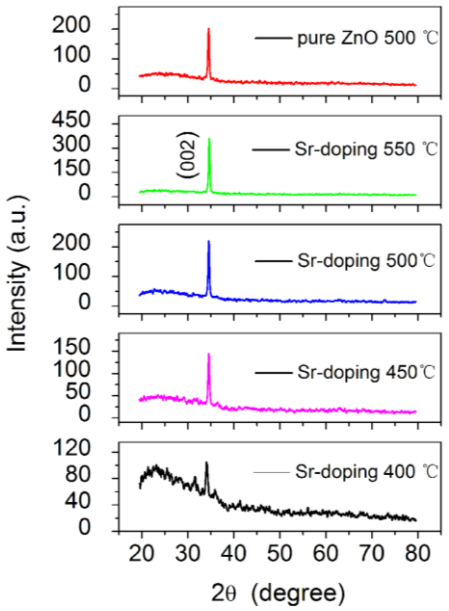

Fig. 1. XRD patterns of the samples

Fig. 2. displays surface and section morphology images of the Sr-doped ZnO thin films annealed at different temperatures. The pure ZnO thin film has uniform grains, dense structure and smooth surface. However, all the Sr-doped ZnO thin films show a porous feature and these pores not only distribute on the film surface but also nearly throughout the whole films. This kind of special porous structure is favorable for film applications in photocatalytic degradation and chemical sensing. With the rise of annealing temperature, both the porosity and average pore size gradually increase. When the annealing temperature rises to 500 ℃, the porosity of the film reaches the maximum. However, when the annealing temperature is further increased, the porosity and pore size decrease again. This probably means that 500 ℃ is the optimal annealing temperature for obtaining a maximum porosity in Sr-doped ZnO thin films. With the increase of annealing temperature, the variation of the porosity in Sr-doped ZnO thin films is mainly connected with the special interactions between the films and substrate interface due to the different thermal energy as well as the lattice distortion originating from Sr-doping [28]. Previously, Teng et al. [28] found that the morphology of the Tb doped ZnO thin films was significantly changed with the rise of annealing temperature; they deemed that the morphology change was induced by Tb-doping and annealing treatment. From Fig. 2 (i), it can be seen that there are some small grains to appear on the Sr-doped ZnO thin film annealed at 550 ℃, while the similar phenomena is not observed for other films. Therefore, the occurrence of these small grains should result from higher annealing temperature. The high-temperature annealing caused the second growth of ZnO thin films. The similar results have been reported by others. For instance, Chen et al. [29] prepared In-doped ZnO thin films by sol-gel method. When the In-doped ZnO thin films were annealed at temperatures above 600 ℃, some rod-like structures occurred on the film surface, which resulted from the recrystallization and growth of ZnO thin films. Furthermore, the film thickness of all the Sr-doped ZnO thin films increases compared with that of the pure ZnO thin film as shown in sectional morphology images. This is mainly induced by the porous structures of the Sr-doped ZnO thin films.

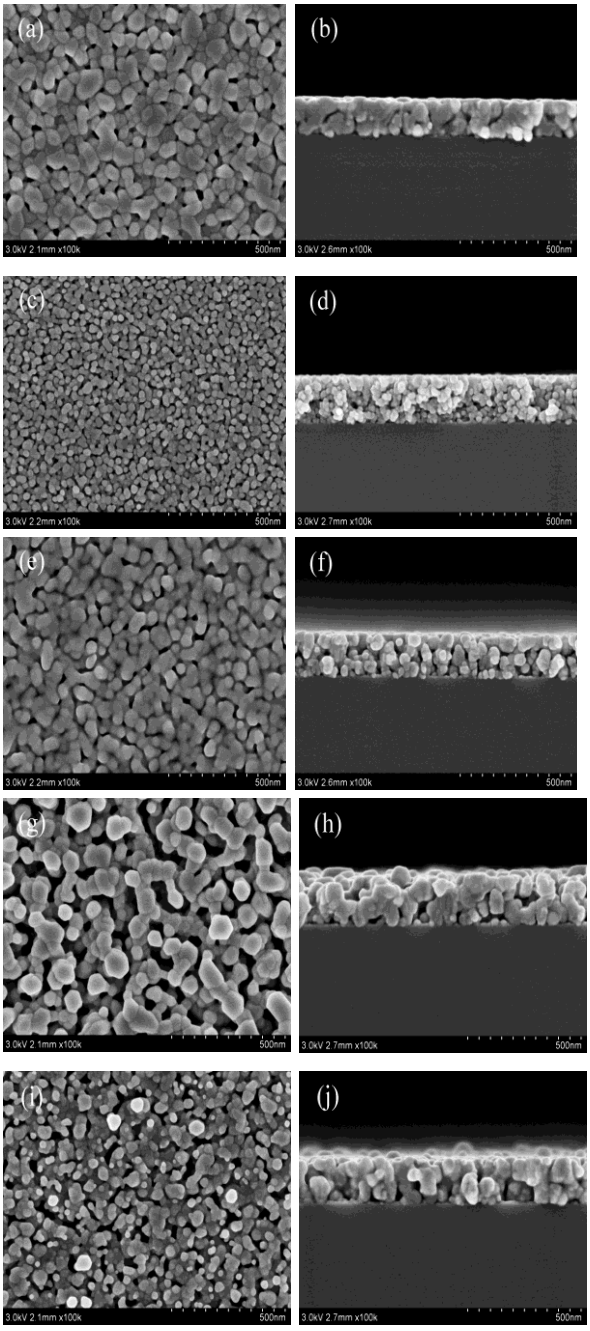

Fig. 2. Surface and section morphology images of the pure ZnO thin film (a, b), and Sr-doped ZnO thin films annealed at 400 ℃ (c, d), 450 ℃ (e, f), 500 ℃ (g, h) and 550 ℃ (i, j)

Fig. 3 shows a typical EDX spectrum of the Sr-doped ZnO thin film. Besides Zn, O and Sr, there are still the signals of C and Si in the spectrum. The C should originate from CO_2 or CO absorbed on the film surface and Si should originate from the Si substrate. The above result means that the deposited ZnO thin films in this study are very pure.

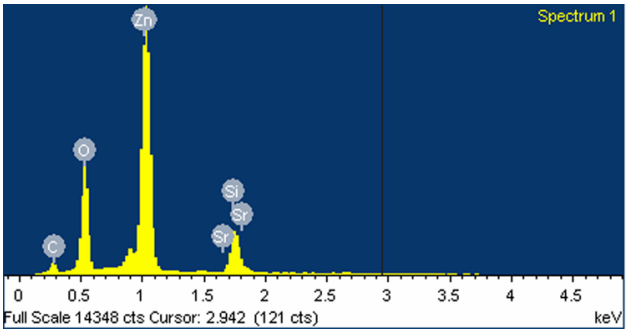

(a)

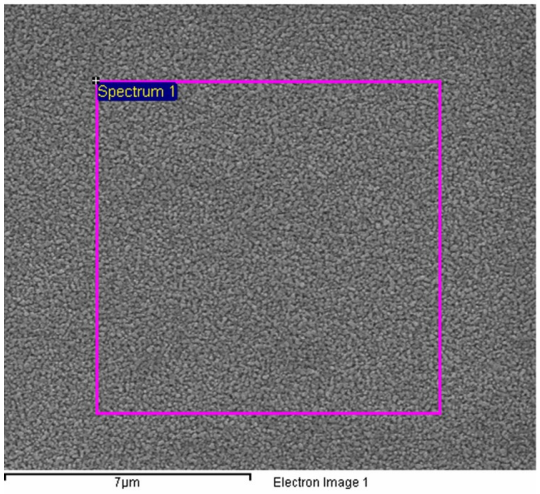

(b)

Fig. 3. A typical EDX spectrum (a) and the surface region of the Sr-doped ZnO thin film (b)

3.2. The photocatalytic activity of the Sr-doped ZnO thin films with various annealing temperatures

Fig. 4 gives the transmittance spectra of the films. The pure ZnO thin film and Sr-doped ones annealed at 400 and 450 ℃ all show high transmittance in the visible range as well as a sharp absorption edge at 375 nm or so. The absorption edge is almost perpendicular to the horizontal axis, implying a direct transition of electrons between conduction band and valence band. With the further increase of annealing temperature, the transmittance of Sr-doped ZnO thin films in the visible range decreases. This is mainly because the porosity is largely enhanced. The higher porosity leads the incident light to be more scattered inside the films, in turn leading more light to be absorbed. Compared with the Sr-doped ZnO thin film annealed at 500 ℃, the pure ZnO thin film displays higher transparency since it has a dense structure, smooth surface and uniform grains.

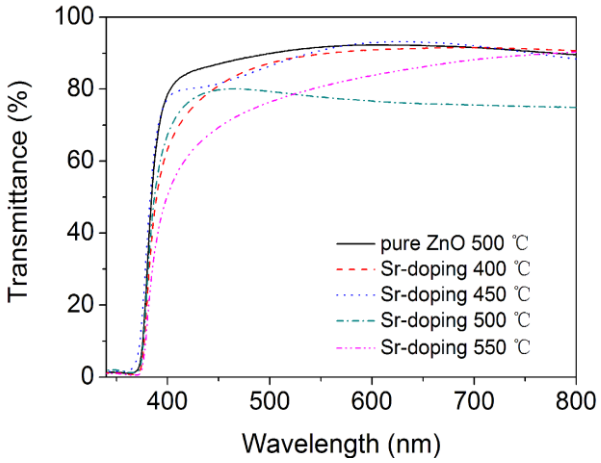

Fig. 4. Transmittance spectra of the samples

In order to investigate the photocatalytic performance of the porous ZnO thin films, the photocatalytic degradation of MB was performed. Fig. 5 (a) exhibits the plots of MB absorbance vs degradation time using the Sr-doped ZnO thin film annealed at 400 ℃ as a photocatalyst and (b) gives the degradation rate of all the samples. It can be seen form Fig. 5 (a) that MB in the solution is decomposed gradually with the extension of reaction time. After photodegradation is carried out for 120 min, all the porous ZnO thin films achieve higher degradation rate than the pure ZnO thin film. This should be ascribed to that the porous structure increases the specific surface area of the films so that the porous films can contact more organic pollutants. Furthermore, the more surface active sites due to Sr-doping are probably also another factor for enhanced photocatalytic performance [14]. The Sr-doped ZnO thin film annealed at 500 ℃ obtains the highest degradation rate of 82%, which is far above that of pure ZnO thin films. It is related with three factors: (1) higher porosity makes the film annealed at 500℃ have higher specific surface area, which in turn leads it to contact more pollutants; (2) the photoinduced carriers are easier to move to grain surface, decreasing the probability of recombination inside the film; (3) the pores are almost throughout the whole films rather than on the film surface, leading more light to be absorbed due to more scattering inside the film. All these factors resultantly let the sample annealed at 500 ℃ obtain the highest degradation rate.

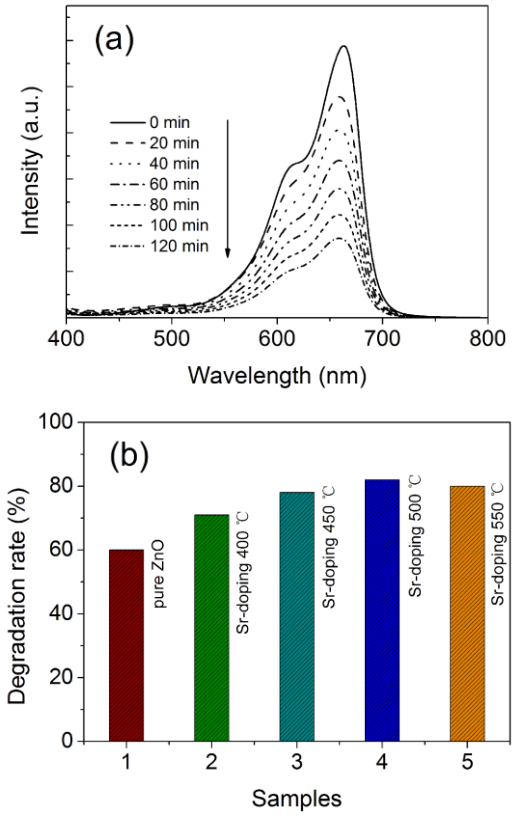

Fig. 5. The absorption spectra of MB solution at different reaction time (a) and degradation rates of the ZnO thin films (b)

In order to quantitatively evaluate the characteristic of the photocatalytic reaction of the films, the kinetics is studied based on photocatalytic degradation of MB. Fig. 6(a) shows the change of C/C_0 with the increase of degradation time, and (b) gives the values of $\ln C/C_0$ at different degradation time. It is clear that the photocatalytic reaction in the MB solution obeys the first-order kinetics and it can be simply described by the following formula [30]:

$$\ln (C/C_0) = - t \quad (2)$$

Where C_0 is the initial concentration of MB, C is the MB concentration after the photocatalytic reaction is performed for t minutes, t is the reaction time, k is the degradation rate constant. The calculated degradation rate constants are listed in table 1, from which it can be seen that the Sr-doped ZnO thin film annealed at 500 ℃shows the highest degradation rate constant.

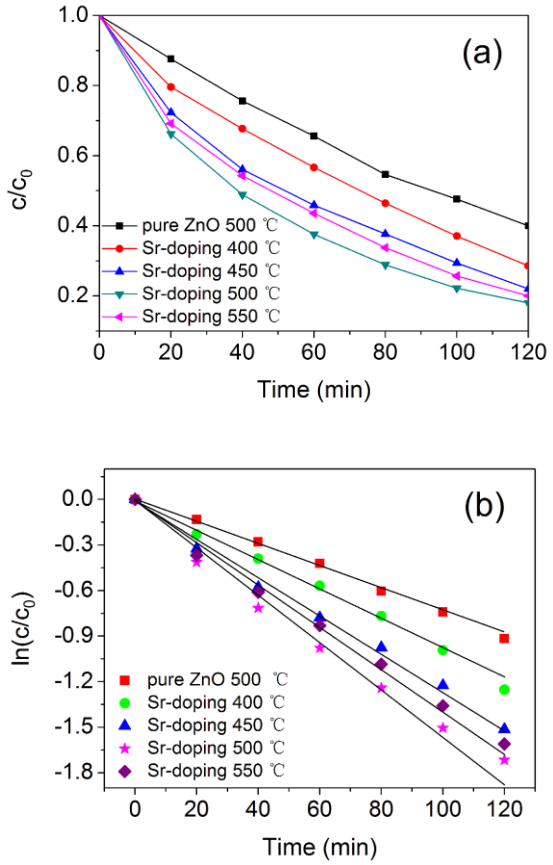

Fig. 6. The plots of C/C_0 and $\ln(C/C_0)$ vs reaction time (t) of the samples

Table 1. The calculated reaction rate constant of the films

Sample	Pure ZnO 500℃	Sr-doping 400℃	Sr-doping 450℃	Sr-doping 500℃	Sr-doping 550℃
k (min^{-1})	0.0076	0.0098	0.0126	0.0155	0.0138

All the above results suggest that annealing the Sr-doped ZnO thin film at 500 ℃ is a feasible method for obtaining porous ZnO thin film with high photocatalytic activity.

4. Conclusion

In this work, a facile method for fabrication of porous ZnO thin films is explored. The results show that for the Sr-doped porous ZnO thin films, the porosity will change with the increasing annealing temperature; the sample annealed at 500 ℃ possesses the highest porosity. The feature of the porous structure is that it not only distributes on the film surface but also nearly throughout the whole film. As a result, the special porous structure greatly enhances the specific surface area, making the film contact more pollutants. Furthermore, the special porous structure induces more scattering of incident light and increases light absorption, resulting in more photoinduced carriers. The photocatalytic degradation of MB demonstrates that these porous ZnO thin films possess good photocatalytic performance.

Acknowledgements

This work is supported by an Open Project Program of Labs in Nanjing University of Information Science and Technology in 2016 (16KF013) and the Natural Science Foundation of the Jiangsu Higher Education Institutions of China (Grant no. 16KJB430021). Dr. Jing Su thanks the financial support by the National Natural Science Foundation of China (Grant no.51472123).

References

[1] A. C. Cakir, P. Guloglu, M. Bilgin, S. Erten-Ela, J. Optoelectron. Adv. M. **14**, 230 (2012).
[2] Bin Zhao, Chun-Ling Wang, Yu-Wen Chen, Hui-Lan Chen, Mater. Chem. Phys. **121**, 1 (2010).
[3] Chao Zhang, Jing Zhang, Yanjie Su, Minghan Xu, Zhi Yang, Yafei Zhang, Physica E **56**, 251 (2014).
[4] Wei Lv, Bo Wei, Lingling Xu, Yan Zhao, Hong Cao, Jia Liu, Appl. Surf. Sci. **259**, 557 (2012).
[5] Weijie Cai, Pilar Pamirez de la Piscina, Narcis Homs, Appl. Catal. B **145**, 56 (2014).
[6] Linhua Xu, Shaorong Xiao, Chengyi Zhang, Gaige Zheng, Weifeng Rao, Fenglin Xian, et al., J. Optoelectron. Adv. M. **16**, 1285 (2014).
[7] Hoda S. Hafez, Physica E **44**, 1522 (2012).
[8] V. Kandavelu, H. Kastien, K. Ravindranathan Thampi, Appl. Catal. B **48**, 101 (2004).
[9] M. Movahedi, A. R. Mahjoub, S. Janitabar-Darzi, J. Iran. Chem. Soc. **6**, 570 (2009).
[10] R. M. Mohamed, Mohamed Abdel Salam, Mater. Res. Bull. **50**, 85 (2014).
[11] Ali Akbar Ashkarran, Bahareh Mohammadi, Appl. Surf. Sci. **342**, 112 (2015).
[12] M. Rezaei, A. Habibi-Yangjeh, Appl. Surf. Sci. **265**, 591 (2013).
[13] M. Faisal, Sher Bahadar Khan, Mohammed M. Rahman, Aslam Jamal, M. M. Abdullah, Appl. Surf. Sci. **258**, 7515 (2012).
[14] Dan Li, Jian-Feng Huang, Li-Yun Cao, Jia-Yin Li, Hai-Bo OuYang, Chun-Yan Yao, Ceram. Int. **40**, 2647 (2014).
[15] T. G. Kele Carvalho, C. Suzane Fidelis, F. Osmando Lopes, Caue Ribeiro, Ceram. Int. **41**, 10587 (2015).
[16] N. Kaneva, I. Stambolova, V. Blaskov, Y. Dimitriev, S. Vassilev, C. Dushkin, J. Alloys Compd. **500**, 252 (2010).
[17] N. Talebian, M. Reza Nilforoushan, N. Maleki, Thin Solid Films **527**, 50 (2013).
[18] Shuhua Dong, Kejing Xu, Juncheng Liu, Hongwei Cui, Physica B **406**, 3609 (2011).
[19] M. Boshta, M. O. Abou-Helal, D. Ghoneim, N. A. Mohsen, R. A. Zaghlool, Surf. Coat. Technol. **205**, 271 (2010).
[20] Wei Xie, Yuanzhi Li, Wei Sun, Jichao Huang, Hao Xie, Xiujian Zhao, J. Photochem. Photobiol. A **216**, 149 (2010).
[21] N. Talebian, M. Reza Nilforoushan, Z. Salehi, Ceram. Int. **38**, 4623 (2012).
[22] B. Pal, M. Sharon, Mater. Chem. Phys. **76**, 82 (2002).
[23] Lina Wang, Yingying Zheng, Xiaoyun Li, Wenjun Dong, Weihua Tang, Benyong Chen, Chaorong Li, Xiao Li, Tierui Zhang, Wei Xu, Thin Solid Films **519**, 5673 (2011).
[24] Huihu Wang, Shijie Dong, Ying Chang, Xiaoping Zhou, Xinbin Hu, Appl. Surf. Sci. **258**, 4288 (2012).
[25] Szu-Ko Wang, Ting-Chun Lin, Sheng-Rui Jian, Jenh-Yih Juang, Jason S.-C. Jang, Jiun-Yi Tseng, Appl. Surf. Sci. **258**, 1261 (2011).
[26] N. R. Aghamalyan, I. A, Gambaryan, E. Kh Goulanian, R. K. Hovsepyan, R. B. Kostanyan, S. I. Petrosyan, E. S. Vardanyan, A. F. Zerrouk, Semicond. Sci. Technol. **18**, 525 (2003).
[27] Shou-Yi Kuo, Wei-Chun Chen, Chin-Pao Cheng, Superlattices Microstruct. **39**, 162 (2006).
[28] X. M. Teng, H. T, Fan, S. S. Pan, C. Ye, G. H. Li, J. Appl. Phys. **100**, 053507 (2006).
[29] K. J. Chen, F. Y. Hung, S. J. Chang, S. Y. Young, Z. S. Hu, Curr. Appl. Phys. **11**, 1243 (2011).
[30] P. Jongnavakit, P. Amornpitoksuk, S. Suwanboon, N. Ndiege, Appl. Surf. Sci. **258**, 8192 (2012).

*Corresponding author: congyu3256@sina.com